

# High verticality InP/InGaAsP etching in Cl<sub>2</sub>/H<sub>2</sub>/Ar inductively coupled plasma for photonic integrated circuits

John S. Parker,<sup>a)</sup> Erik J. Norberg, Robert S. Guzzon,  
Steven C. Nicholes, and Larry A. Coldren

Department of Electrical and Computer Engineering, University of California, Santa Barbara,  
California 93106

(Received 1 September 2010; accepted 3 November 2010; published 5 January 2011)

High verticality and reduced sidewall deterioration of InP/InGaAsP in Cl<sub>2</sub>/H<sub>2</sub>/Ar inductively coupled plasma etching is demonstrated for a hydrogen dominant gas mixture. Selectivity >20:1, an etch rate of 24 nm/s, and a sidewall slope angle of >89° have been measured for etch depths >7 μm. The Ar flow is minimized to reduce surface etch damage while increased Cl<sub>2</sub> and H<sub>2</sub> gas flow is shown to increase etch rate and selectivity. The high chamber pressure required for plasma ignition causes isotropic etching at the start and creates an undercut beneath the masking layer. A novel ignition scheme using a hydrogen gas “flood” is suggested and results are presented. © 2011 American Vacuum Society. [DOI: 10.1116/1.3522659]

## I. INTRODUCTION

In photonics, deeply etched waveguides provide high confinement to the optical mode allowing for tight bends with low radiation losses. Dry etching can achieve such high-aspect ratio structures in InP/InGaAs,<sup>1,2</sup> InP/InGaAlAs,<sup>1</sup> and InP/InGaAsP<sup>2</sup> with vertical sidewalls and minimal discontinuities between the various layers. These structures can be made with a single etch-step and typical etch rates >20 nm/s.<sup>3</sup> Recently, an 8×8 monolithic tunable router with more than 200 functional elements has been demonstrated, which combined deeply etched, surface ridge, and buried rib waveguides.<sup>4</sup> As future applications continue to increase the number of components on photonic integrated circuits (PICs), the component size will need to be further reduced and more of them will rely upon the deeply etched platform to achieve compact structures with tight bends.

To realize high yield on large PICs, the dry-etch process must produce uniform and vertical structures to ensure that waveguide and component widths are conserved from the lithography, which is critical to minimize insertion loss. One functional element that is highly sensitive to waveguide width variations is the four-port restricted multimode interference (MMI) coupler<sup>5</sup> used heavily for integrated power splitters, combiners, and Mach-Zehnder interferometers (MZIs). For example, from three-dimensional beam propagation method (BPM) simulations using Rsoft BEAMPROP software, the acceptable width tolerance is <120 nm to achieve <1 dB insertion loss on a typical 8.1 μm wide, 100 μm long, restricted MMI as shown in Fig. 1. This requires a sidewall slope angle >88.6° to match the average waveguide width to the mask dimensions within 120 nm, assuming the middle of the waveguide is 2.5 μm below the mask layer (300 nm height waveguide, 1.8 μm p-InP cladding, 150 nm contact layer, and 400 nm InP cap). If reproducible coupling and low insertion loss cannot be obtained in MMI couplers,

the extinction ratio in Mach-Zehnder interferometers will be decreased, and the performance of MZI modulators and balanced detectors will be degraded.

As an additional requirement, the sidewall surface of the waveguide must be smooth to reduce scattering losses that have significant effect for tight bending radii <100 μm. A variety of photonic components have been previously demonstrated with a deeply etched process including ring resonators,<sup>6</sup> slot couplers,<sup>7</sup> MMI couplers,<sup>8</sup> distributed Bragg reflector gratings,<sup>9</sup> and photonic crystals.<sup>10</sup>

Inductively coupled plasma (ICP) reactive ion etching (RIE) has become widespread for etching InP based structures. Elevated electrode temperatures (>150 °C) are commonly used to increase the volatility of the InCl<sub>x</sub> byproducts and reduce micromasking.<sup>11</sup> Etching with only Cl<sub>2</sub> gas has been shown to produce smooth sidewalls with selectivity of 20:1 for a SiN<sub>x</sub> or SiO<sub>2</sub> mask.<sup>9</sup> While Berg and Pang<sup>12</sup> has shown a much higher selectivity for InP of >300:1 using a less common Ti/Ni mask, their feature sizes and etch depths were relatively large (i.e., >10 and >69 μm, respectively), and their process required long etch times of 110 min. However, the Cl<sub>2</sub> chemistry generally suffers from a large undercut or slow anisotropic etch rates.<sup>2</sup> Dry-etch Cl<sub>2</sub>-based chemistries with additive gas including Cl<sub>2</sub>/Ar,<sup>2,13</sup> Cl<sub>2</sub>/H<sub>2</sub>,<sup>3,14–16</sup> Cl<sub>2</sub>/H<sub>2</sub>/Ar,<sup>2,9–11,17,18</sup> Cl<sub>2</sub>/O<sub>2</sub>,<sup>19</sup> Cl<sub>2</sub>/N<sub>2</sub>,<sup>20,21</sup> and Cl<sub>2</sub>/BCl<sub>3</sub>/N<sub>2</sub>,<sup>22</sup> have been studied previously to improve anisotropy and etch rate.

Adding Ar to the Cl<sub>2</sub> based chemistry benefits etch anisotropy due to an increased physical etch component from Ar ion bombardment. Gatilova *et al.*<sup>14</sup> and Bouchoule *et al.*<sup>15</sup> showed that when using a Si carrier with Cl<sub>2</sub>-based chemistry, a SiO<sub>x</sub> passivation layer forms on the semiconductor sidewall and is enhanced by H<sub>2</sub> gas, further improving anisotropic etching. Selectivity of 30:1 has been found etching with Cl<sub>2</sub>/H<sub>2</sub> chemistry,<sup>3</sup> while Cl<sub>2</sub>/H<sub>2</sub>/Ar selectivity remains around 14:1 using a SiO<sub>2</sub> mask.<sup>9</sup> The downside of Cl<sub>2</sub>/H<sub>2</sub> etching is that good verticality has only been demonstrated for chamber pressures ≤1 mT,<sup>3</sup> which is not available on all

<sup>a)</sup>Electronic mail: jpark@ece.ucsb.edu

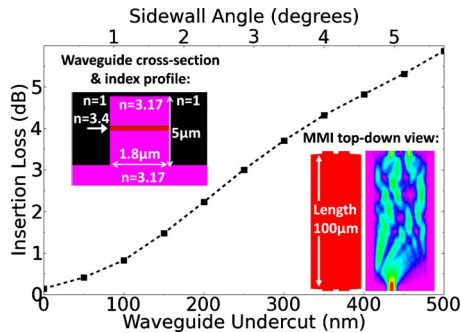


FIG. 1. (Color online) Rsoft BPM simulation of MMI coupler insertion loss vs waveguide undercut due to nonvertical etching. The reduction of the waveguide width greatly increases the insertion loss. The restricted MMI design is  $100\ \mu\text{m}$  in length and has an optimal width of  $8.1\ \mu\text{m}$  for  $1.8\ \mu\text{m}$  input waveguides.

systems, while  $\text{Cl}_2/\text{H}_2/\text{Ar}$  provides anisotropic etches at pressures as high as 4 mTorr with a greater process tolerance.<sup>9–11</sup> In studies with other additive gas besides Ar or  $\text{H}_2$ ,  $\text{Cl}_2/\text{O}_2$  based chemistry shows higher verticality than with only  $\text{Cl}_2$  due to  $\text{O}_2$  surface passivation. Selectivity of  $>13:1$  was observed with a  $\text{SiN}_x$  mask; however, micro-masking at high  $\text{O}_2$  ratios remains a limitation of this chemistry.<sup>19</sup> In etch studies on high-aspect ratio holes for photonic crystals,  $\text{N}_2$  is commonly used as a passivation gas added to  $\text{Cl}_2$  based chemistry providing higher verticality and reduced sidewall deterioration.<sup>20,21</sup>  $\text{BCl}_3$  has been reported to form more reactive chlorine ions than  $\text{Cl}_2$ , and the investigation of  $\text{BCl}_3$  added to the  $\text{Cl}_2/\text{N}_2$  based chemistry has shown a further improved verticality while causing increased sidewall roughness.<sup>22</sup> Selectivity for  $\text{Cl}_2/\text{N}_2$  based chemistry with a  $\text{SiN}_x$  mask is reported to be quite low compared to other chemistries at  $>8:1$ .<sup>20–22</sup> However, these measurements are taken on photonic crystals, which have a large RIE lag effect reducing the InP etch rate in small sub-micrometer features, and therefore this etch selectivity cannot be directly compared to etches on waveguides or electronic components.

Starting from previous work by Rommel *et al.*<sup>2</sup> using 2/2.5/3 SCCM (SCCM denotes cubic centimeter per minute at STP) ( $\text{Cl}_2/\text{H}_2/\text{Ar}$ ) and Docter *et al.*<sup>9</sup> using 7/11/4 SCCM ( $\text{Cl}_2/\text{H}_2/\text{Ar}$ ), we show that a higher  $\text{H}_2$  gas ratio improves verticality, and that increased total gas flow improves selectivity and etch rates while maintaining extremely vertical sidewalls. One predominant form of etching damage observed for  $\text{Cl}_2/\text{H}_2$  based chemistry is an undercut notch directly beneath the mask layer.<sup>1</sup> In functional InP/InGaAsP PICs, the undercut notch can damage the contact layer, typically InGaAs, which is near the top of the layer stack and close to the etch mask. Extensive plasma damage to the contact layer can produce surface traps and an increased contact resistance. In this article, we present an optimized high gas flow recipe for  $\text{Cl}_2/\text{H}_2/\text{Ar}$  ICP that has the highest selectivity, etch rates, and verticality yet reported. In addition, we demonstrate that a hydrogen gas “flood” can reduce the undercut notch, and that compensation of total etch area is necessary when etching small InP pieces.

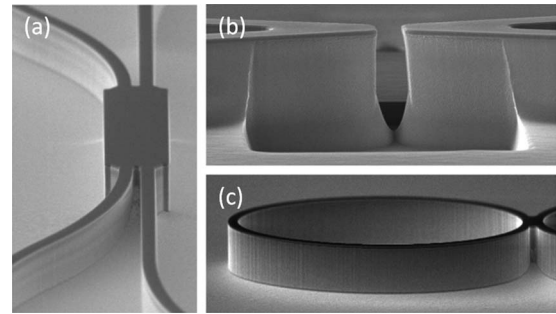


FIG. 2. SEM images of various dry etched photonic components including (a) multimode interference coupler, (b) etched beam splitter coupler, and (c) ring resonator with a compact two-mode coupler.

## II. EXPERIMENTAL SET UP

Etching studies were performed on InP:S wafers with a metalorganic chemical vapor deposition grown 350 nm thick 1.4Q InGaAsP waveguide, seven InGaAsP quantum wells and barriers, and an InGaAs:Zn contact layer. A three-level mask is used to define the deeply etched photonic patterns that include the following: 550 nm of plasma-enhanced chemical vapor deposition  $\text{SiO}_2$  on the InP/InGaAsP sample, followed by 50 nm Cr, and 900 nm photoresist (PR) SPR955CM-0.9 defined by stepper lithography. The Cr is etched in a Panasonic E640 ICP with a nonheated low power  $\text{Cl}_2$  based recipe with a PR-to-Cr selectivity of 1:1. The PR is removed and the  $\text{SiO}_2$  mask is defined in the Panasonic E640 ICP with a nonheated low power  $\text{SF}_6$ -based dry-etch recipe with  $\text{SiO}_2$ -to-Cr selectivity of 30:1. The Cr mask is removed by repeating the same low power  $\text{Cl}_2$  based Cr etch recipe. No InP damage was observed in scanning electron microscope (SEM) images after this etch. The resulting  $\text{SiO}_2$  mask is nearly vertical ( $\sim 86^\circ$  sidewall slope) compared to a typical  $\text{SiO}_2$  masked etched with  $\text{CHF}_3$  chemistry ( $\sim 66^\circ$  sidewall slope). The more vertical mask profile reduces InP sidewall deterioration during the etch, which is common on sloped mask profiles as the tapered edges of the mask layer break down.

The InP etching was done in a Unaxis Versalock (VLR) ICP RIE chamber with a  $200\ ^\circ\text{C}$  heated chuck and backside He cooling to regulate the temperature. Samples are loaded on a 4 in. Si carrier wafer that is necessary to avoid micromasking<sup>11</sup> and to develop the  $\text{SiO}_x$  passivation layer needed for anisotropic etching;<sup>15</sup> no thermal grease is used to adhere the samples to the carrier. Figure 2 shows several InP components deeply etched on this tool including the following: a ring resonator with a compact two-mode coupler, a MMI coupler, and a slot coupler. During the fabrication of these components, we found high etch rates and smooth sidewalls around 800–850 W ICP/125 W RIE, and we used these power conditions for this gas flow study. A series of tests was conducted on  $\sim 1\ \text{cm}^2$  InP/InGaAsP pieces cleaved from two larger samples (sample A used for 850 W ICP experiments and sample B for 800 W ICP experiments). In order to avoid edge effects and improve the etch uniformity across the sample, InP pieces with a total area of  $4\ \text{cm}^2$  (i.e.,

TABLE I. H<sub>2</sub> and Cl<sub>2</sub> gas flow variations at 800 and 850 W ICP power. All etches done on 1 cm<sup>2</sup> InP/InGaAsP sample with 4 cm<sup>2</sup> chamber loading and 300 min etch time. Sidewall angle measurements taken at the maximum waveguide undercut.

ICP/RIE (W)	Gas flows (SCCM)				Cl <sub>2</sub> /H <sub>2</sub> (%)	Etch rate (nm/s)	Selectivity (InP:SiO <sub>2</sub> )	Sidewall
	Total	Cl <sub>2</sub>	H <sub>2</sub>	Ar				Angle off Vertical (deg)
800/125	30	7	21	2	33	19	16	0.4–0.7
800/125	30	8	20	2	40	20.5	18	0.5–0.8
800/125	30	9	19	2	47	24	20.5	0.5–0.8
800/125	29	9	18	2	50	22.5	19	0.4–0.7
800/125	27	10	15	2	67	21.5	18	0.4–0.7
850/125	21	4.75	14.25	2	33	18	16	1–1.3
850/125	21	6.3	12.6	2	50	17	15	3–3.3
850/125	29	9	18	2	50	21.5	18.5	0.8–1.1
850/125	40	12.6	25.2	2	50	27	23	0.9–1.2
850/125	78	25.2	50.4	2	50	39	24	~33 <sup>a</sup>
850/125	21	7.6	11.4	2	67	20	17	4.5–4.8

<sup>a</sup>Features greatly undercut and damaged due to high chamber pressure. Angle measurement was made at the upper undercut.

“chamber loading” samples) are placed evenly around the sample and are reused for each 300 min etch test.

### III. RESULTS AND DISCUSSION

#### A. Etch rates, selectivity, and verticality

The most optimal etch conditions were found to be 800 W ICP, 125 W RIE with gas flows of 9 SCCM Cl<sub>2</sub>, 19 SCCM H<sub>2</sub>, and 2 SCCM Ar for a chamber pressure of 1.5 mTorr. Table I shows the results of the gas composition study for the 850 W ICP and 800 W ICP tests. SEM images of the corresponding waveguide cross-sections are shown in Figs. 3 and 4. As listed in Table I, the reduction in ICP power from 850 to 800 W shows only a minor improvement in the verticality, which is already >89° for the 9/18/2 (Cl<sub>2</sub>/H<sub>2</sub>/Ar) test at 850/125 W (ICP/RIE). The 2 SCCM Ar flow used in all of the experiments was found to be necessary for creating stable plasma ignition; increased Ar ratio in the gas chemistry results in reduced selectivity and deeper vertical striations on the sidewalls due to the increased physical etch caused by Ar ion bombardment. The optimal H<sub>2</sub> gas fraction found on the Unaxis VLR for vertical sidewalls is 62%–66% of the total flow, which is a different operating regime than previously studied by Rommel *et al.*<sup>2</sup> using 23%–33% H<sub>2</sub> on a PlasmaTherm SLR 770 and Docter *et al.*<sup>9</sup> using 50% H<sub>2</sub> on an Oxford Plasma Technology 100, indicating that the ideal gas ratios are reactor specific. This is further supported by the different dc-bias voltages used by Rommel (–215 V), Docter (–150 to –420 V), and in this study (–115 V at 800 W ICP and –111 V at 850 W ICP). For a fixed distance between electrodes, a higher dc-bias produces a greater electric field causing ions to reach a higher velocity. Thus, at lower dc-biases, etching becomes more chemically dependent as physical bombardment is reduced.

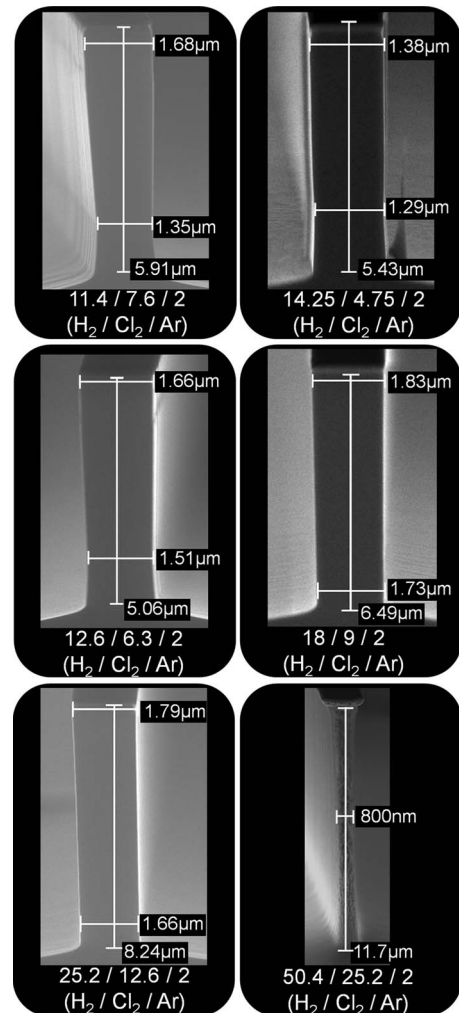


FIG. 3. SEM images of waveguide cross-sections for etch gas composition variations at 850/125 W (ICP/RIE).

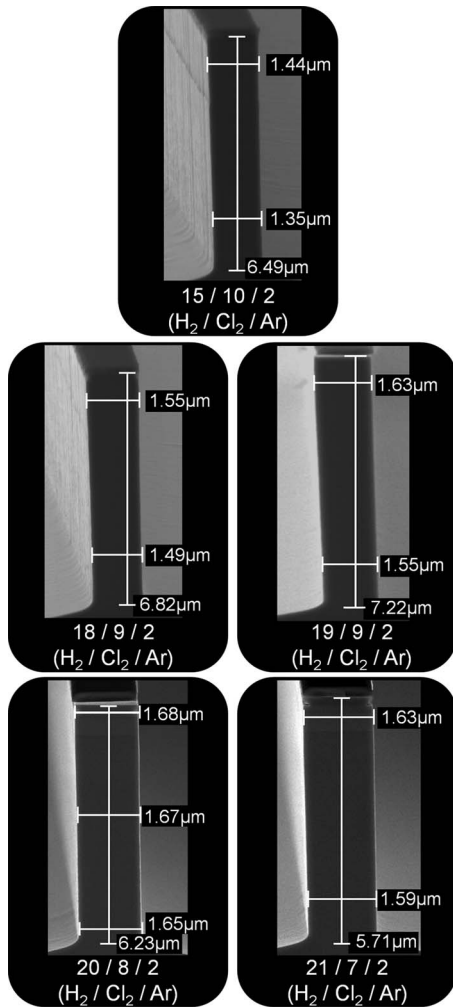


FIG. 4. SEM images of waveguide cross-sections for etch gas composition variations at 800/125 W (ICP/RIE).

Higher  $\text{Cl}_2/\text{H}_2$  gas flow is found to increase etch rate and improve selectivity as shown in Table I. For 850/125 W (ICP/RIE) with 6.3/12.6/2 SCCM ( $\text{Cl}_2/\text{H}_2/\text{Ar}$ ), the etch rate is 17 nm/s and selectivity of 15:1, whereas at double the hydrogen and chlorine 12.6/25.2/2 SCCM ( $\text{Cl}_2/\text{H}_2/\text{Ar}$ ), the etch rate has increased to 27 nm/s and selectivity to 23:1. However, above 30 SCCM total gas flow, the pump on our system cannot maintain the 1.5 mTorr set-point. This occurs in the run 12.6/25.2/2 SCCM ( $\text{Cl}_2/\text{H}_2/\text{Ar}$ ) in which the chamber pressure is set at 1.5 mTorr, but the turbo-vacuum maintained  $\sim 2$  mTorr during the etch. Even with this chamber pressure increase, the sidewall verticality was still quite good indicating that 2 mTorr is still a sufficiently low pressure for vertical etching. Eventually, the verticality is reduced as increased gas flow causes the chamber pressure to rise above 2 mTorr. For instance, with 25.2/50.4/2 SCCM ( $\text{Cl}_2/\text{H}_2/\text{Ar}$ ), the chamber pressure rose to  $\sim 6$  mTorr during the etch and significant undercut occurred causing the thin 12  $\mu\text{m}$  tall waveguide to break in many places. All systems will have an upper limit to their selectivity and total

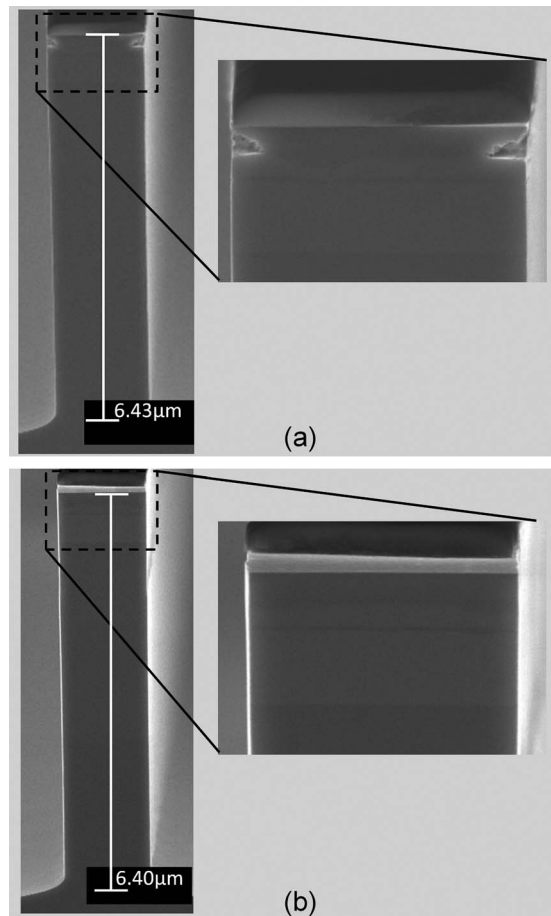


FIG. 5. SEM images of the waveguide cross-section (a) with the standard high pressure ignition process causing isotropic etching, and (b) with the improved ignition process using a hydrogen gas flood before ignition to passivate the InP and followed by hydrogen gas reduction after ignition to speed up the transition to low chamber pressure.

etch rate determined by the pump. In this series of experiments, sidewall slopes  $>89^\circ$  were obtained only for pressures  $\leq 2$  mTorr during the etch.

## B. Reduction of sidewall damage

An undercut notch  $>100$  nm deep is visible directly below the  $\text{SiO}_2$  mask in Fig. 5(a), which has appeared in most of our etches regardless of chemistry and has been found in other InP etch studies.<sup>1</sup> This undercut notch is especially troublesome as most active InP devices have a  $p$ -contact layer beneath the mask which would be damaged by such a notch. The notch is caused by the inability of the vacuum system to open the throttle-valve and reduce the chamber pressure rapidly after the high pressure ignition at 20 mTorr and 500/15 W (ICP/RIE). High pressure ignition above 10 mTorr is common on ICP systems. While additional rf electrodes, magnetic fields, and ultraviolet ion excitation could improve ignition at lower pressure, these capabilities are rarely found in ICP tools. At such high ignition pressures, the etch is isotropic and etches underneath the mask during the 10–20 s, the vacuum controller takes to stabilize the pressure



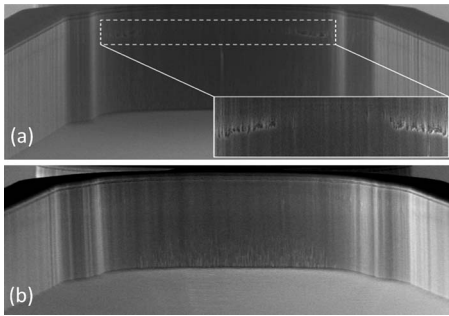


FIG. 6. SEM image of (a) sidewall pitting on small etch area of  $\sim 5 \text{ cm}^2$  and (b) smooth sidewalls without pitting after  $4 \text{ cm}^2$  of added chamber loading.

below 2 mTorr for high verticality anisotropic etching. The notch is further enhanced without the protective  $\text{SiO}_x$  passivation layer at the etch start.

In order to address the notch, we start the  $\text{Cl}_2$  and  $\text{H}_2$  flows at 4/20 SCCM, respectively. This “hydrogen flood” causes the turbovac throttle-valve to open, and after ignition, the high-hydrogen ratio helps to promote the formation of the  $\text{SiO}_x$  passivation layer.<sup>14</sup> After ignition occurs, the hydrogen gas flow is reduced to 8 SCCM, which helps the chamber pressure to drop rapidly to 1.5 mTorr for anisotropic etching. Once the pressure is stabilized at 1.5 mTorr, a gas ramp brings the  $\text{Cl}_2$  and  $\text{H}_2$  flows up to 9/19 SCCM over 20 s while maintaining their flow ratio. An etched sample with the modified gas ignition steps shows no notch as seen in Fig. 5(b).

Pitting defects have also been observed on various features on small etch samples with area  $< 5 \text{ cm}^2$ . These defects contribute to scattering loss and occur often on waveguide bends with very small radii. The cause of this pitting is unknown, but might be due to localized build-up of excess gas reactants. Since the samples being etched are much smaller than the Si carrier wafer, nonuniform gas concentrations may be formed over the sample. Increasing the etch area with the addition of chamber loading pieces was found to alleviate the occurrence of pitting. Figure 6(a) shows waveguide pitting in small bending radius structures for initial test etches with an area  $\sim 5 \text{ cm}^2$ . Chamber loading samples were added in  $\sim 2 \text{ cm}^2$  increments until pitting was no longer observed. This occurred with  $\sim 9 \text{ cm}^2$  of total etch area as shown in Fig. 6(b).

#### IV. CONCLUSION

The etch verticality was improved by optimizing the gas ratios for 800–850 W ICP power. For maximum selectivity and etch rate, the total  $\text{Cl}_2$  and  $\text{H}_2$  gas flow should be set as high as possible for a given ratio while maintaining a constant chamber pressure  $\leq 2$  mTorr. The Ar flow should be set as low as possible while maintaining stable plasma conditions. The optimal flows of 9/19/2 SCCM ( $\text{Cl}_2/\text{H}_2/\text{Ar}$ ) produced selectivity  $> 20:1$ , an etch rate of 24 nm/s, and a sidewall angle of  $89.2^\circ$ – $89.5^\circ$ . High pressure conditions at plasma ignition often result in a notch beneath the etch mask.

Plasma ignition using a hydrogen flood scheme was shown to prevent these undercut notches. Pitting of the InP/InGaAsP sidewalls has been observed when etching small pieces with area  $\leq 5 \text{ cm}^2$  and can be corrected by adding chamber loading samples to increase the amount of etched material in the chamber.

#### ACKNOWLEDGMENTS

The authors wish to thank Demis John for assistance with the  $\text{SF}_6$  etch of  $\text{SiO}_2$ . This work was supported by the Office of Naval Research. A portion of this work was done in the UCSB nanofabrication facility, part of the NSF funded NNIN network.

- <sup>1</sup>S. Guilet, S. Bouchoule, C. Jany, C. S. Corr, and P. Chabert, International Conference on Indium Phosphide and Related Materials, Princeton, NJ, 7–11 May 2006 (unpublished), Paper No. WB2.3, p. 262.
- <sup>2</sup>S. L. Rommel *et al.*, J. Vac. Sci. Technol. B **20**, 1327 (2002).
- <sup>3</sup>S. Guilet, S. Bouchoule, C. Jany, C. S. Corr, and P. Chabert, J. Vac. Sci. Technol. B **24**, 2381 (2006).
- <sup>4</sup>S. C. Nicholes, M. L. Mašanović, B. Jevremović, E. Lively, L. A. Coldren, and D. J. Blumenthal, J. Lightwave Technol. **28**, 641 (2010).
- <sup>5</sup>M. Bachmann, P. A. Besse, and H. Melchior, Appl. Opt. **34**, 6898 (1995).
- <sup>6</sup>E. J. Norberg, R. S. Guzzon, S. C. Nicholes, J. S. Parker, and L. A. Coldren, IEEE Photonics Technol. Lett. **22**, 109 (2010).
- <sup>7</sup>E. J. Norberg, J. S. Parker, U. Krishnamachari, R. S. Guzzon, and L. A. Coldren, Conference on Integrated Photonics and Nanophotonics Research and Applications, Honolulu, HI, 12–17 July 2009 (unpublished), Paper No. IWA1.
- <sup>8</sup>J. S. Parker, Y. Hung, E. J. Norberg, R. S. Guzzon, and L. A. Coldren, Conference on Integrated Photonics and Nanophotonics Research and Applications, Honolulu, HI, 12–17 July 2009 (unpublished), Paper No. IWA2.
- <sup>9</sup>B. Docter, E. J. Geluk, M. J. H. Sander-Jochem, F. Karouta, and M. K. Smit, Symposium IEEE/LEOS Benelux, Eindhoven, The Netherlands, 30 October 2006 (unpublished), p. 97.
- <sup>10</sup>F. Karouta, B. Docter, A. A. M. Kok, E. J. Geluk, J. J. G. M. van det Tol, and M. K. Smit, Electrochemical Society Fall Meeting, Honolulu, HI, 12–17 October 2008 (unpublished), Paper No. E5, p. 987.
- <sup>11</sup>F. Karouta, B. Docter, E. J. Geluk, M. J. H. Sander-Jochem, J. J. G. M. van det Tol, and M. K. Smit, Annual Meeting of the Lasers and Electrochemical Society, Sydney, Australia, 23–27 October 2005 (unpublished), Paper No. ThDD2.
- <sup>12</sup>E. W. Berg and S. W. Pang, J. Electrochem. Soc. **146**, 775 (1999).
- <sup>13</sup>R. J. Shul, G. B. McClellan, R. D. Briggs, D. J. Rieger, S. J. Pearton, C. R. Abernathy, J. W. Lee, C. Constantine, and C. Barratt, J. Vac. Sci. Technol. A **15**, 633 (1997).
- <sup>14</sup>L. Gatilova, S. Bouchoule, S. Guilet, and P. Chabert, J. Vac. Sci. Technol. A **27**, 262 (2009).
- <sup>15</sup>S. Bouchoule, G. Patriarche, S. Guilet, L. Gatilova, L. Largeau, and P. Chabert, J. Vac. Sci. Technol. B **26**, 666 (2008).
- <sup>16</sup>G. A. Curley, L. Gatilova, S. Guilet, S. Bouchoule, G. S. Gogna, N. Sirse, S. Karkari, and J. P. Booth, J. Vac. Sci. Technol. A **28**, 360 (2010).
- <sup>17</sup>W. Zhao, J. W. Bae, I. Adesida, and J. H. Jang, J. Vac. Sci. Technol. B **23**, 2041 (2005).
- <sup>18</sup>J. H. Jang, W. Zhao, J. W. Bae, D. Selvanathan, S. L. Rommel, I. Adesida, A. Lepore, M. Kwakernaak, and J. H. Abeles, Appl. Phys. Lett. **83**, 4116 (2003).
- <sup>19</sup>C. F. Carlström, R. van der Heijden, F. Karouta, R. W. van der Heijden, H. W. M. Salemink, and E. van der Drift, J. Vac. Sci. Technol. B **24**, L6 (2006).
- <sup>20</sup>J. W. Bae, C. H. Jeong, J. T. Lim, H. C. Lee, G. Y. Yeom, and I. Adesida, J. Korean Phys. Soc. **50**, 1130 (2007).
- <sup>21</sup>R. van der Heijden *et al.*, Symposium IEEE/LEOS Benelux, Ghent, Belgium, 2–3 December, 2004 (unpublished), p. 287.
- <sup>22</sup>K. H. Lee, S. Guilet, G. Patriarche, I. Sagnes, and A. Talneau, J. Vac. Sci. Technol. B **26**, 1326 (2008).